LAWRENCE
LIVERMORE
NATIONAL
LABORATORY

LLNL-TR-648636

Analysis of a Uranium Oxide Sample Interdicted in Slovakia (FSC 12-3-1)

Lars E. Borg, Zurong Dai, Gary R. Eppich, Amy M. Gaffney, Victoria G. Genetti, Patrick M. Grant, Leonard W. Gray, Kiel S. Holiday, Ian D. Hutcheon, Theresa M. Kayzar, Gregory L. Klunder, Kimberly B. Knight, Michael J. Kristo, Rachel E. Lindvall, Naomi E. Marks, Christina E. Ramon, Erick C. Ramon, Martin Robel, Sarah K. Roberts, Kerri C. Schorzman, Michael A. Sharp, Michael J. Singleton, Ross W. Williams

Lawrence Livermore National Laboratory

January 23, 2014

Disclaimer

Auspices Statement

This work performed under the auspices of the U.S. Department of Energy by Lawrence Livermore National Laboratory under Contract DE-AC52-07NA27344.

Abstract

We provide a concise summary of analyses of a natural uranium sample seized in Slovakia in November 2007. Results are presented for compound identification, water content, U assay, trace element abundances, trace organic compounds, isotope compositions for U, Pb, Sr and O, and age determination using the $^{234}U - ^{230}Th$ and $^{235}U - ^{231}Pa$ chronometers. The sample is a mixture of two common uranium compounds - schoepite and uraninite. The uranium isotope composition is indistinguishable from natural; ^{236}U was not detected. The O, Sr and Pb isotope compositions and trace element abundances are unremarkable. The $^{234}U - ^{230}Th$ chronometer gives an age of 15.5 years relative to the date of analysis, indicating the sample was produced in January 1997. A comparison of the data for this sample with data in the Uranium Sourcing database failed to find a match, indicating the sample was not produced at a facility represented in the database.

Introduction

This report documents the analysis of a natural uranium sample seized in Pribenik, eastern Slovakia on 28-November 2007. The Police of the Slovak Republic seized 481.4 g of radioactive material (Figure 1). The radioactive material was smuggled from Ukraine with the intention to sell it to a "customer" for an asking price of $1300 USD per gram. The sample was initially analyzed in the Dept. of Nuclear Chemistry at the University of Comenius, Bratislava and determined to have an isotopic composition consistent with natural uranium. In March 2008, the Nuclear Regulatory Authority of the Slovak Republic organized transport of a ~5g aliquot of the sample to the European Union's Joint Research Center/ITU Karlsruhe for detailed analysis. The analyses at ITU confirmed the initial results while providing additional information on the ^{236}U content, less than 0.000012%, and age, 10.4 ± 0.4 years, i.e., the sample was last chemically purified in June 2007.

Through the assistance of the U.S. Dept. of State, a ~20 g aliquot of the sample was transferred to Lawrence Livermore National Laboratory (LLNL) on 23 February 2012 for a comprehensive nuclear forensic analysis. The results of these analyses are presented herein.

Fig. 1. Photograph of interdicted uranium oxide sample in Slovakia.

Analytical Methods

Since the material appeared homogeneous, approximately 1 g was removed for analysis and split into aliquots. Moisture content was determined by heating at 140 C for 14 hours. The analytical procedure began with XRD analyses, followed by dissolution of several aliquots that were analyzed for morphology, trace elements, U, Pb, and Sr isotopes, and chronology. A separate aliquot was used for O-isotope analysis.

The phase composition of the samples was determined by X-ray diffraction (XRD). The samples were top loaded as slurry onto a zero background silicon plate imbedded in a Poly methyl methacrylate (PMMA) sample holder. The samples were analyzed on a Bruker AXS D8 ADVANCE X-ray diffractometer equipped with a LynxEye 1-dimentional linear Si strip detector; DIFFRACplus Evaluation package Release 2009 software was used for data analysis. X-ray fluorescence analysis (XRF) was performed using a Bruker AXS S8 Tiger. X-ray photoemission spectroscopy (XPS) was performed on a PHI Quantum 2000 system using a focused monochromatic Al Kα X-ray source (1486.6 eV) for excitation and a spherical analyzer with 16-element multichannel detection system. Binding energies were referenced to the C 1s photoelectron line arising from adventitious carbon at 284.8 eV and charge neutralization was achieved with low energy electrons and ions. Curve fitting of overlapping peaks are achieved with MULTIPAK 9.2 (PHI) curve fitting routines with asymmetric or Gaussian-Lorentzian line-shapes and a Shirley background. Grain morphology was determined with an FEI Inspect FE-SEM equipped with a Kevex EDS x-ray system.

A visible/NIR spectrometer (Analytical Spectral Devices, Inc.) equipped with three separate detectors that spanned consecutive spectral regions: 350 – 1000 nm (Vis+), 1000 – 1800 nm (NIR1), and 1800 – 2500 nm (NIR2) was used for optical spectroscopy. The light source was a 20W tungsten-halogen lamp. A bifurcated fiber-optic bundle was used to transmit light to the sample surface, collect the reflected light, and return it to the spectrometer. Some measurements required a lens to couple the light to the sample at a longer standoff distance. Each analysis consisted of an average of 10 scans over the complete range of the spectrometer, 350 – 2500 nm. Five analyses were performed on each sample, with each analysis interrogating a different surface location of the same sample. Data reduction and analysis were performed using the Unscrambler X ver. 10.1(CAMO Software AS). Data pretreatment by standard normal variate transformation, a common correction for reflectance measurements, was applied to the data to remove interferences due to scatter and particle size effects, and also center the data on zero. Principal component analysis of the different spectral regions highlighted the sample differences.

Trace element abundances were determined using a Thermo Electron X7 quadrupole ICP-MS. Acid digestions of ~0.1 grams of the sample powder were diluted in a HNO_3/HF solution to a U concentration of ~180 ppmw. A Rh internal standard was added prior to analysis for internal calibration. Total uranium content and the uranium isotopic composition were measured on the samples using mass spectrometry after dissolution in HNO_3/HF. Gravimetric dilutions of the solutions were spiked with ^{233}U and analyzed by high-resolution multi-collector inductively coupled plasma-mass spectrometry (MC-ICP-MS, Nu Plasma) for total uranium content (by isotope dilution mass spectrometry (IDMS)) and uranium isotope composition. The isotopic composition of Sr was determined using a Triton thermal ionization mass spectrometer after purification on Sr-spec resin. The Sr data were corrected for mass bias (instrument fractionation) using $^{86}Sr/^{88}Sr = 0.1194$. Lead was separated using AG-1X anion resin and HBr and HCl acids. The Pb fraction was analyzed using HR MC-ICP-MS (Nu-Plasma). Pb isotopic results were

corrected for mass bias using Tl added to the sample immediately prior to mass spectrometry analysis, using a $^{205}Tl/^{203}Tl$ value of 2.3875. The oxygen isotope composition was analyzed on a Prism III gas source mass isotope ratio spectrometer (IRMS). Oxygen from the sample was liberated by reaction with ClF_3 gas at 550 C and then converted to CO_2 prior to IRMS analysis. Oxygen isotope compositions are reported as per mil values relative to Vienna Standard Mean Ocean Water (VSMOW).

Age dating (the time since last chemical purification) was performed using the ^{234}U – ^{230}Th chronometer. Dissolutions of FSC 13-2-1-B-1 through B-3 were spiked with ^{233}U and ^{229}Th. U and Th were then radiochemically separated, purified, and measured by MC-ICPMS (Nu Plasma). The concentration of ^{230}Th relative to ^{234}U were used to calculate a model age [10, 11] based upon the assumption that all Th was removed from the sample during processing and that the material remained a closed system afterwards (i.e., no loss or addition of Th). ^{228}Th was measured (at LLNL) using alpha spectrometry for the ^{228}Th – ^{232}Th isotope chronometer. Organic species were collected via solid-phase microextraction (SPME) and subsequent analysis by gas chromatography/mass spectrometry (GC/MS). Volatile and semi-volatile compounds in were sampled using a 65-µm PDMS/DVB SPME fiber. Approximately 1 g of U oxide in a 20-ml septum vial, as well as a process blank, were heated in an aluminum block on a hot plate at 65 ºC for 15 minutes prior to performing a 30-minute SPME collection in the vial headspace. After sample exposure, the SPME fibers were desorbed at 250ºC for 3 minutes and analyzed by GC/MS using a 30-m, HP-5ms column with 0.25-mm inner diameter and 0.25-µm film thicknesses. The temperature of the GC oven was programmed as follows: 30º C for 3 minutes, ramped at 6º C/min to 280º C, and maintained at 280º C for 3 minutes. The MS was scanned from *m/z* = 29 -550 amu. Organic components were identified using AMDIS (Automated Mass Spectral Deconvolution and Identification System, ver. 2.66, August 2008) and the NIST Mass-Spectral Library (2011).

Phase composition

The analytical results are shown in Table 1 and Figure 2. The analyses demonstrate that the sample is roughly 60% schoepite and 40% uraninite with a minor amount of studite.

Table 1 – Analytical X-ray diffraction results for FSC-12-31-B

	Name	Formula	Approximate Percent Abundance
Major Phase	Schoepite	$((UO_2)_8O_2(OH)_{12})\bullet 12(H_2O)$	60%
Minor Phase	Uraninite	UO_2	40%

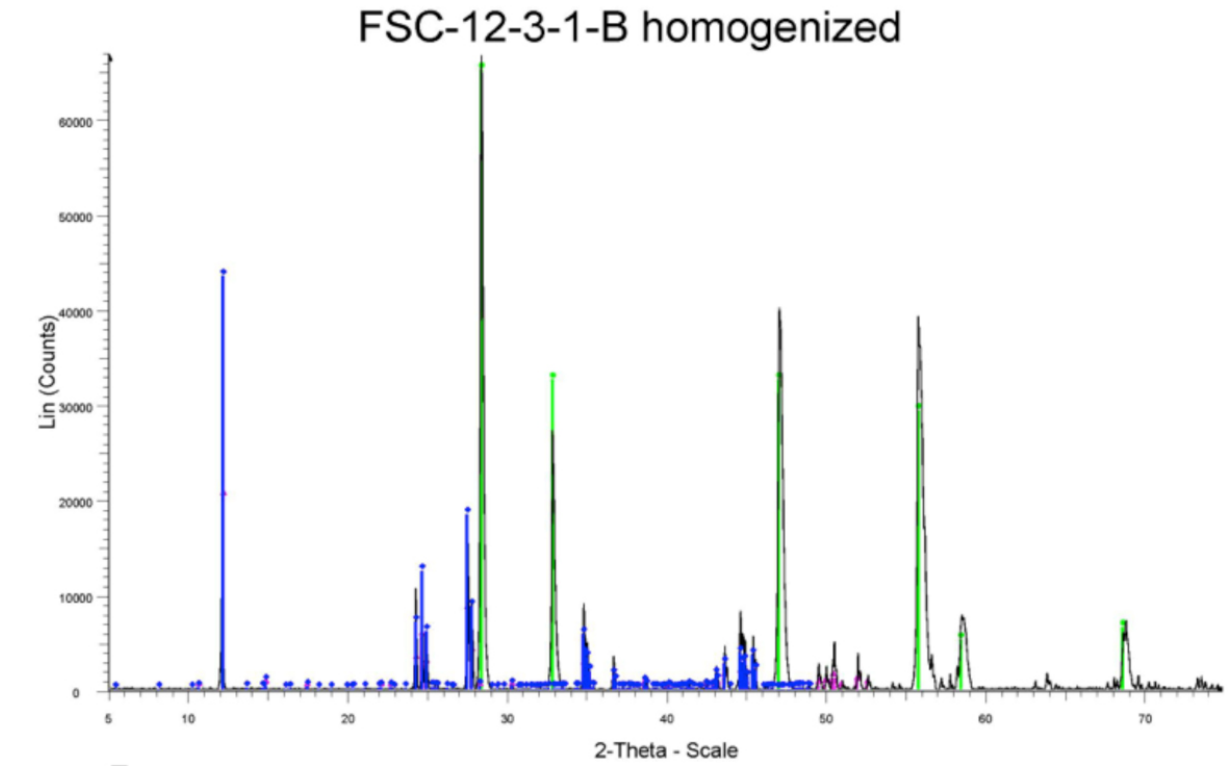

Figure 2 – X-ray diffraction analysis of FSC-12-3-1-B. Black trace shows data for FSC 12-3-1; green and blue lines indicate peak positions for schoepite and studite, respectively.

Optical Spectroscopy

The sample is a black powder as shown in the white light photo in Figure 3.

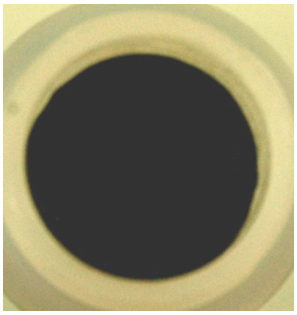

Figure 3. Photo of FSC 12-3-1.

The diffuse reflectance spectrum for this sample over the range of 350-2500 nm is presented in Figure 4. The spectrum is separated into 3 sections corresponding to the 3 detectors in the spectrometer. The Vis+ region, which covers up to 1000 nm, shows a large absorption band that spans the visible range from 400-700 nm with a smaller band 820 nm. In order to compare this sample to others in the database, a standard normal variate (SNV) transformation was applied which normalizes the data and minimizes particle size effects. A principal component analysis (PCA) of the SNV applied to Vis+ spectra in the database provided the scores plot shown in Appendix 2. The different UOC materials were identified based on the XRD major phase

determinations and are color coded as per the figure caption. In general there is good separation of the different classes, however, there is some overlap particularly for U_3O_8 and UO_2. When sample 12-3-1 is predicted by projecting onto the PCA plot, it lies close to the U_3O_8/UO_2 cluster. This assignment is consistent with the visual observations of color and further discrimination cannot be made.

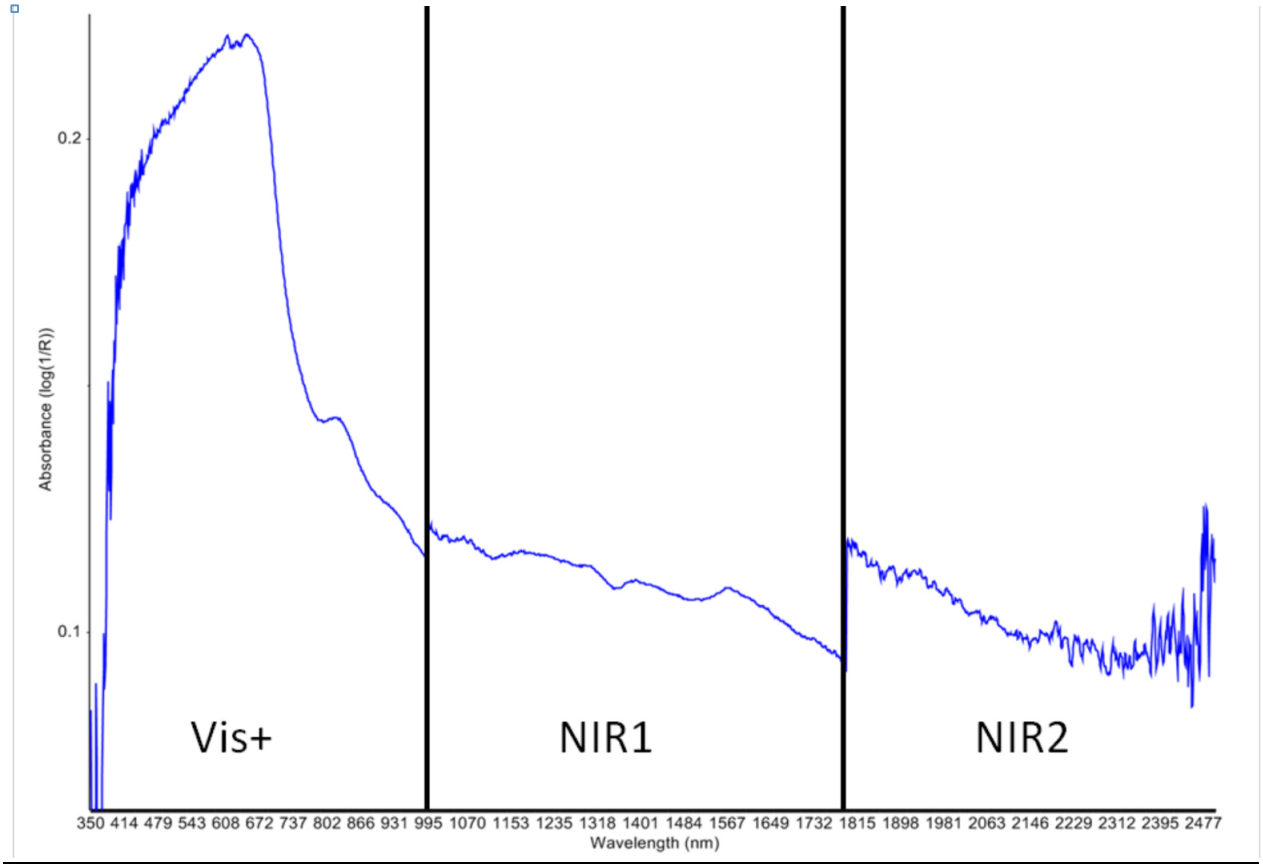

Fig. 4. Diffuse reflectance spectra of sample FSC 12-3-1 over the wavelength range from 350-2500 nm; see test for a description of the bands.

Morphology

SEM/EDS examination reveals two characteristic morphologies – tablets roughly 2 to 10 μm in linear dimension and 0.4 – 0.7 μm thick and a fine-grained agglomeration of nanometer scale (50-200 nm) particulates (Fig. 5). The agglomerates themselves are assembled into platelets similar in shape to the smaller of the compact platelets (Fig. 6). Both morphologies are intimately intergrown to form aggregates 10 – 70 mm across. Close examination of the platelets reveals evidence of incipient breakdown suggesting the aggregates are an alteration product (Fig. 7). A comparison between the SEM/EDS and XRD data shows that the platelets are uraninite (U_3O_8), while the aggregates are schoepite ($(((UO_2)_4O(OH)_{12})\bullet 6(H_2O)$). Schopeite is a known alteration product of uraninite, formed through the action of liquid water.

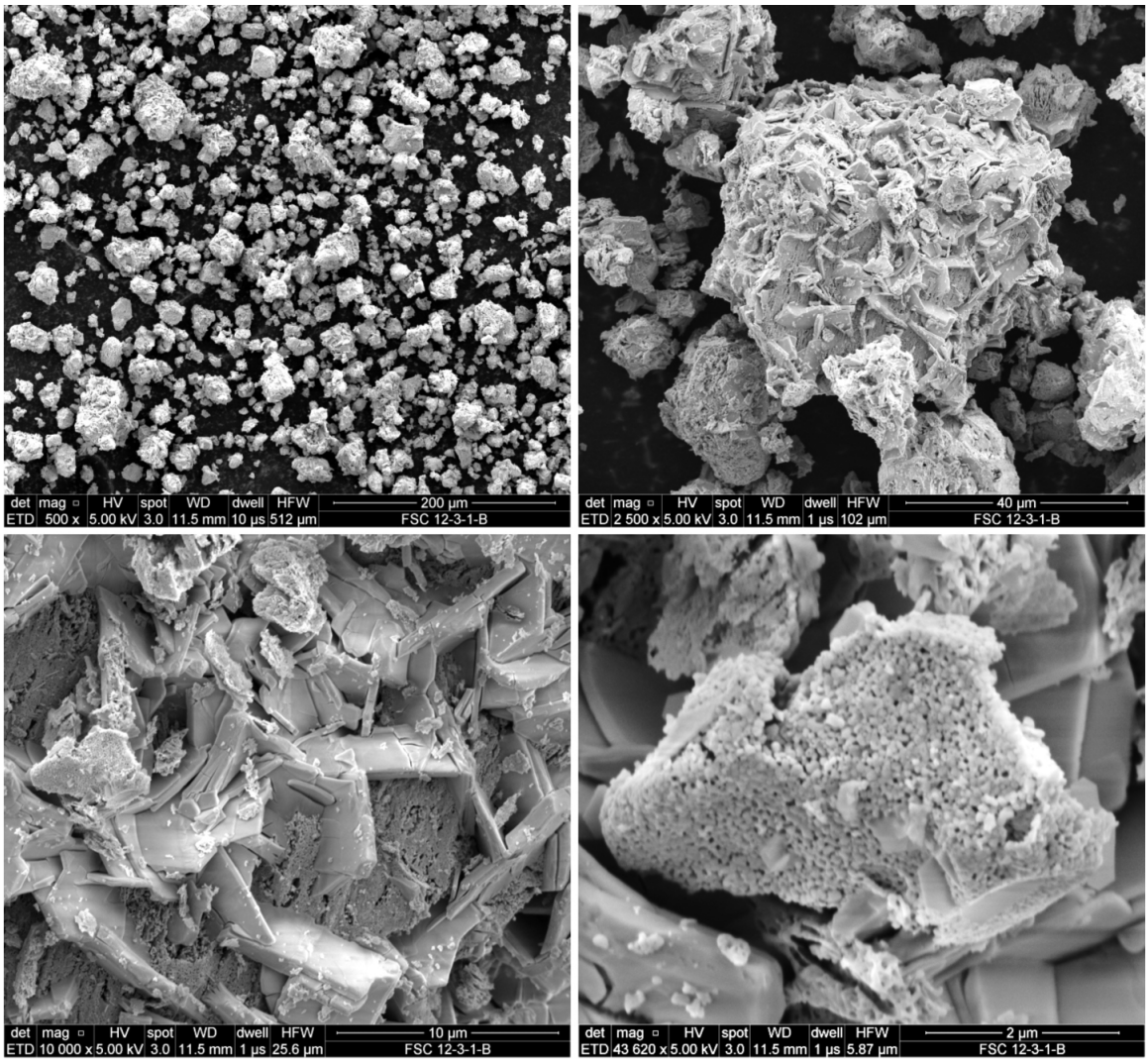

Fig. 5. SEM secondary electron photomicrograph showing characteristic morphologies of FSC 12-3-1. (A) Dispersed particles; scale bar is 200 nm. (B) Close up of aggregate composed of platelets and agglomerated nanometer particles; scale bar is 40 μm. (C) Assembly of platelets and aggregates; scale bar is 10 μm. (D) Close up view of an agglomeration of nanometer scale particulates assuming the habit of the parent platelet; scale bar is 2 μm.

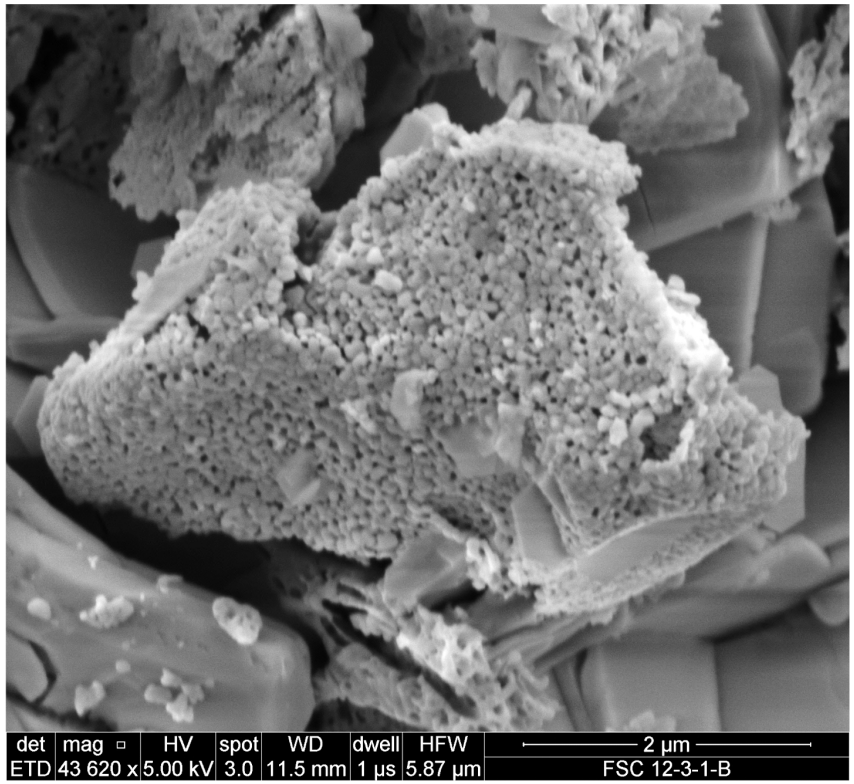

Fig. 6. SEM secondary electron photomicrograph showing nanometer scale particulates assuming the habit of the larger uraninite platelets. This behavior suggests schoepite formed as an alteration product of uraninite. Scale bar is 2 μm.

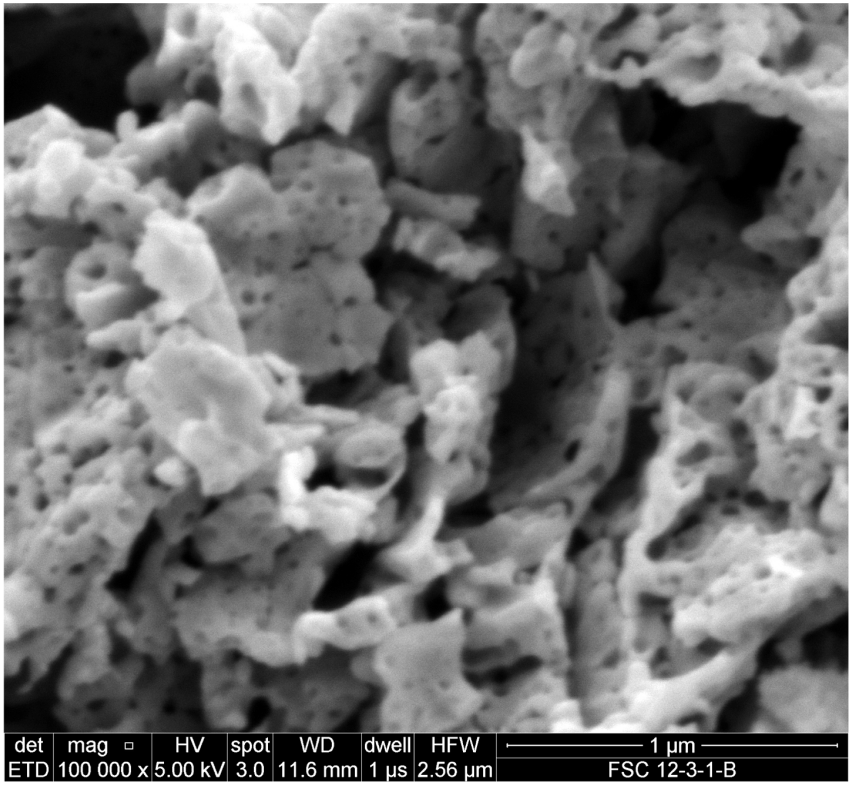

Fig. 7. SEM secondary electron photomicrograph showing incipient breakdown of uraninite to form schoepite, note the development of porosity. Scale bar is 1 μm.

Oxidation State

The X-ray photoelectron spectrometry analyses confirm the XRD analyses demonstrating the bulk sample is primarily UO_2 (Figure 8). This spectrum demonstrates the presence of adventitious carbon that is almost always unrelated to sample composition. Exposed surface areas of grains appear to have been oxidized to higher uranium oxidation states, such as U_4O_9 and U_3O_7.

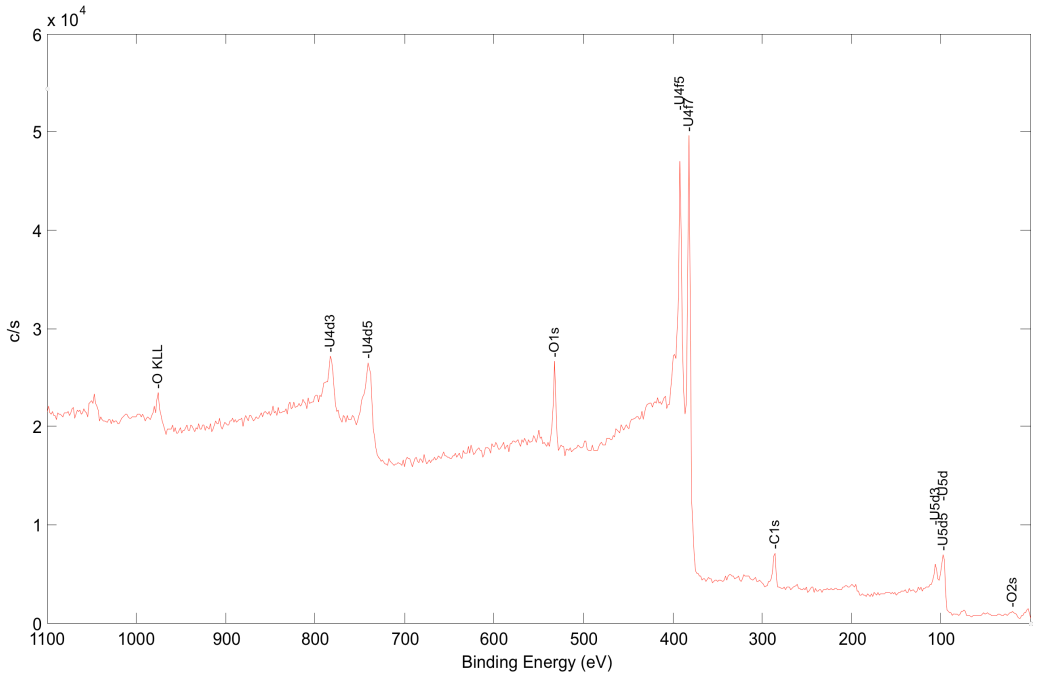

Figure 8. Survey XPS spectrum of 12-3-1 identifying uranium oxide containing adventitious carbon typical of powdered samples.

Moisture content

The moisture content was determined by weight loss after heating the sample to 140 ^{0}C for 14 hours. The value of 2.65 ± 0.05 wt.% represents the average of three independent measurements.

Uranium content

The uranium content was determined by isotope dilution mass spectrometry after the sample had been heated to 140^{0}C to remove water. This procedure was completed on three separate aliquots, giving U contents ranging from 83.2 to 86.9 wt.%. The average value of 84.5 ± 2.4 wt.% is consistent with a mixture of schoepite and studite.

Trace element composition

Trace element composition of FSC 12-3-1 is presented below in (Table 2). This sample is relatively pure but contains significant quantities of Fe (160 ppm), Ca (86 ppm), Mo (80 ppm), Al (52 ppm), Pb (41 ppm), and Na (40 ppm). Rare earth element (REE) abundances are very

low (<< 1 μg/g) and were not sufficiently above detection limits to constrain the REE pattern of the sample.

Table 2. Trace element abundances

Element	Concentration (μg/g U)	Uncertainty k=3	Element	Concentration (μg/g U)	Uncertainty k=3
Be	0.01	0.03	Sn	-0.01	0.05
Na	40	9	Sb	2.3	1.5
Mg	13.1	1.7	Te	-0.01	0.13
Al	52	11	Cs	-0.01	0.08
K	26	12	Ba	1.0	0.1
Ca	86	17	La	0.021	0.013
Ti	3	1.1	Ce	0.024	0.004
V	0.25	0.04	Pr	0.0036	0.0011
Cr	7.2	0.5	Nd	0.012	0.007
Mn	23.9	1.1	Sm	0.006	0.003
Fe	160	20	Eu	0.0018	0.0017
Co	0.055	0.010	Gd	0.008	0.006
Ni	4	0.3	Tb	0.0009	0.0005
Cu	1.3	0.7	Dy	0.004	0.002
Zn	1.6	1.2	Ho	0.0008	0.0004
Ga	-0.157	0.015	Er	0.0025	0.002
Ge	-0.03	0.05	Tm	0.0007	0.0005
As	0.05	0.1	Yb	0.003	0.002
Se	0.04	0.19	Lu	0.0005	0.0005
Rb	0.06	0.07	Hf	0.17	0.02
Sr	0.8	0.07	Ta	0.001	0.005
Y	0.012	0.005	W	0.113	0.018
Zr	17.3	0.7	Re	0.056	0.012
Nb	0.43	0.04	Ir	0.001	0.003
Mo	80	3	Pt	0.004	0.006
Ru	0.004	0.006	Tl	0.023	0.006
Rh	0.0011	0.0013	Pb	41	7
Pd	0.03	0.03	Th	0.036	0.006
Ag	0.12	0.05	Pu	<0.0001	
Cd	0.012	0.019			

1. Negative values are reported in accordance with IAEA guidance for reporting trace element concentrations in uranium ore and ore concentrate.

Isotopic composition: U, Pb, Sr and O

Aliquots were analyzed for U, Pb, Sr, and O isotopic compositions. The uranium isotope composition is indistinguishable from natural and ^{236}U was not detected. The data are presented in Table 3. Lead isotope analyses demonstrate that a nonradiogenic composition similar to most Pb in the Earth's crust. Although not anomalous, the $^{206}Pb/^{204}Pb$ ratio is, however, slightly lower than many crustal rocks (Table 4). Like U and Pb, the Sr isotopic composition is typical of continental crust and many UOC and U-ore samples (Table 5). Finally, the O isotopic

composition of 12-3-1 is $\delta^{18}O$ = -4.0 ± 0.8‰, an unremarkable value for uranium ore concentrate.

Table 3. U Isotopic Composition

U Isotopic Ratio	Value	Uncertainty
$^{234}U/^{238}U$	0.00005473	0.00000015
$^{235}U/^{238}U$	0.0072488	0.0000036
$^{236}U/^{238}U$	$< 3 \times 10^{-8}$	---

Table 4. Pb Isotopic Composition

Pb Isotopic Ratio	Value	Uncertainty
$^{208}Pb/^{204}Pb$	37.3572	0.0066
$^{207}Pb/^{204}Pb$	15.5453	0.0028
$^{206}Pb/^{204}Pb$	17.4520	0.0039

Table 5. Sr Isotopic Composition

Sr Isotopic Ratio	Value	Uncertainty
$^{87}Sr/^{86}Sr$	0.711052	0.000030
$^{84}Sr/^{86}Sr$	0.056484	0.000005

Chronometry

The ^{234}U – ^{230}Th age of the sample was determined on 3 aliquots processed and analyzed separately; the results are presented in Table 6. Separation of U and Th were completed on 24-July 2012 and all ages are calculated relative to this date. Ages determined on the three aliquots range from 15 March 1996 to 10 January 1997 with a typical uncertainty of 0.16 y. Although the ages are in general agreement, they are not concordant within the analytical uncertainty. Sample 12-3-1-B2, which has the oldest apparent age, also has a significantly higher Th content and we believe the most plausible explanation for the discordant ages is contamination with environmental Th (contamination here refers to the introduction of extraneous Th prior to interdiction, most plausibly during the manufacturing process). If we assume aliquot B2 has the same ages as the other aliquots, we can infer the $^{232}Th/^{230}Th$ ratio of the contaminant thorium. The inferred value of $^{232}Th/^{230}Th = 1.39 \times 10^5$ falls within the range of values expected for environmental contaminants. We conclude the sample was produced in early January 1997 with an uncertainty of roughly 2 months. It should be noted that the presence of excess Th introduced by contamination systematically biases ages to values that are too old. We cannot exclude the possibility that the entire sample received by LLNL contains excess Th introduced at the manufacturing facility or during subsequent handling. In this event, the 15.5 year age reported here would represent an upper limit to the true age.

Table 6. ^{230}Th – ^{234}U ages

Sample ID	Reference Date	^{230}Th-^{234}U Model Age (years)	Expanded uncertainty (k=2)	Model Date	Expanded Uncertainty (days)
FSC 12-3-1-B 1	24-Jul-12	15.57	0.15	28-Dec-96	53
FSC 12-3-1-B 2	24-Jul-12	16.35	0.18	15-Mar-96	64
FSC 12-3-1-B 3	24-Jul-12	15.53	0.19	10-Jan-97	68

In addition to ^{234}U – ^{230}Th chronometry, the ^{235}U – ^{231}Pa chronometer was also applied to the samples; the results are presented in Table 7. Ages are calculated using the date of chemical separation, 19-September 2012. Unfortunately, the ages are anomalously old, indicating that that ^{231}Pa was not removed quantitatively at the time the sample was last chemically purified.

Table 7. ^{231}Pa – ^{235}U ages

Sample ID	Reference Date	^{231}Pa-^{235}U Model Age (years)	Expanded uncertainty (k=2)	Model Date	Expanded Uncertainty (days)
FSC 12-3-1-B-1	19-Sep-12	197.1	6.0	ca. 1815	2206
FSC 12-3-1-B-2	19-Sep-12	191.9	6.0	ca. 1820	2155

Organic Compounds

Figure 9 shows the GC-MS chromatogram of FSC 12-3-1-A and the process blank. Peaks present in the blank SPME sample were eliminated from further analysis. After processing, 100 different compounds were concluded to be unique to the sample. These 100 peaks were analyzed using AMDIS, Chemstation and manual interpretation to tentatively identify the multiplicity of species. While AMDIS successfully deconvolutes overlapping spectra, we have found that it often incorrectly reports the presence of several components when only a single compound is present, and likewise often fails to properly identify alkanes because of the very similar spectral features of these compounds. Despite its limitations, however, proper use of AMDIS is a valuable analytic tool that can also provide a common protocol for GC/MS data reduction among independent laboratories. Table 8 shows the tentative identification of the 100 compounds identified in FSC 12-3-1-A. As with several other interdicted uranium oxide samples, the organic compounds provide a unique fingerprint that could be used to link this sample to a second questioned sample, should one become available for analysis. The absence of a more complete understanding of the origin of the organic compounds inhibits the use of this signature for source attribution.

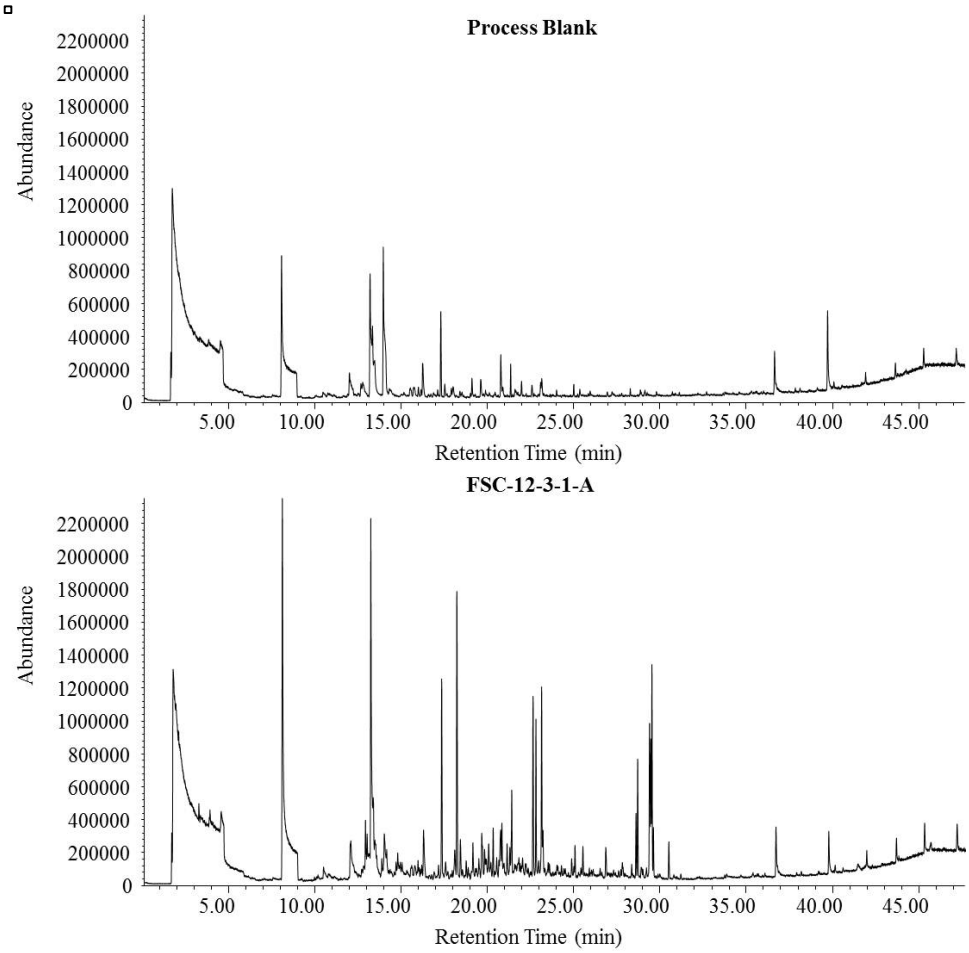

Figure 9. Total ion chromatograms representing a process blank and FSC specimen 12-3-1-A; analyses by SPME PDMS/DVB and GC/MS.

Table 8. Organic components detected in the SPME-GC/MS profile of FSC 12-3-1-A after subtracting the process blank background species.

Peak Number	Retention Time (min)	Tentative ID	Purity	Weighted Match Factor[1]	FSC 12-3-1-A
1	3.85	1-Butanol	10%	90	XX
2	9.91	3-Heptanone	34%	77	x
3	10.11	5-Methyl-1,2,3-thiadiazole	21%	76	x
4	10.71	4-Hydroxybutanoic acid	24%	78	XX
5	12.02	57(100) 77(50) 106(45) 105(44)	30%	68	XX
6	12.67	5-Methyl-pyrimidine	22%	74	XX
7	12.68	Carbonic acid, butyl phenyl ester	10%	73	x
8	12.87	2,2,4,6,6-Pentamethylheptane	71%	93	XX
9	12.96	1,2,4-Trimethylbenzene	46%	92	XX
10	13.41	3-Ethyl-3-methylheptane	13%	75	XX
11	13.51	3,3-Dimethyloctane	36%	81	x
12	13.80	2,2,5-Trimethylhexane	46%	87	x
13	13.81	2,2,4,6,6-Pentamethylheptane	51%	88	XX
14	13.92	2-Ethyl-1-hexanol	5%	91	x
15	14.09	3,7-Dimethyldecane	34%	78	XX
16	14.30	43(100) 55(80) 73(72) 89(40)103(10)	17%	62	x
17	14.63	2,2,4-Trimethylhexane	50%	82	XX
18	14.63	2,6-Dimethyloctane	48%	84	x
19	14.73	4,7-Dimethylundecane	44%	86	XX
20	14.88	2,6,8-Trimethyldecane	20%	71	x
21	14.98	Acetophenone	29%	78	XX
22	15.25	4-Methyl-2,4-bis(4'-trimethylsilyloxyphenyl)pentene	9%	76	x
23	15.90	3-Ethyl-3-methylheptane	36%	82	XX
24	15.91	4,7-Dimethylundecane	41%	81	x
25	15.97	Acetic acid, trichloro-, heptyl ester	27%	70	x
26	16.05	3,3-Dimethylhexane	23%	70	x
27	17.63	57(100) 71(84) 85 (56) 41 (55) 43(50)	26%	57	XX
28	18.03	Azulene	23%	76	XX
29	18.15	1-Dodecene	91%	96	XX
30	18.36	Tridecane	73%	87	XX
31	18.47	N,N-Dimethyl-1,4-benzenediamine	9%	74	XX
32	18.69	3,6-Dimethylundecane	60%	89	XX
33	18.70	2,6-Dimethylundecane	61%	86	x
34	18.81	Benzocycloheptene	29%	71	XX
35	18.88	4,4-Dimethylundecane	32%	75	x
36	19.23	3-Ethyl-3-methylheptane	26%	78	x
37	19.29	1,4-Dimethyl-2-(2-methylpropyl)benzene	22%	76	x
38	19.43	4,6-Dimethyldodecane	48%	84	XX

39	19.60	Undecane	41%	73	XX
40	19.64	(1,3-Dimethylbutyl)benzene	27%	75	XX
41	19.76	O-Decyl-hydroxylamine	64%	76	XX
42	19.82	Hexylbenzene	37%	77	x
43	19.87	57(100) 55(100) 85(76) 71(67) 43(65)	48%	64	XX
44	19.99	1,2,3,4-Tetrahydro-6-methylnaphthalene	14%	79	XX
45	20.08	6,6-Dimethylundecane	22%	71	x
46	20.26	Pentadecane	74%	86	XX
47	20.46	4,7-Dimethylundecane	39%	75	XX
48	20.59	Nonadecane	56%	82	XX
49	20.67	2-Methylnaphthalene	54%	92	XX
50	20.70	Tridecane	49%	90	XX
51	21.07	1-Methylnaphthalene	59%	81	XX
52	21.23	1,2,3,4-Tetrahydro-2,7-dimethylnaphthalene	45%	77	XX
53	21.31	2,6,10-Trimethyldodecane	55%	84	XX
54	21.51	3-Ethyl-3-methylheptane	28%	77	x
55	21.67	4,8-Dimethylundecane	24%	72	XX
56	21.75	71(100) 188(73) 73(60) 57(58) 160(56)	42%	55	XX
57	21.82	57(100) 71(75) 43(39) 160(28)	8%	44	XX
58	21.91	5-Methyltridecane	39%	83	x
59	21.94	1-Methyl-3-hexylbenzene	29%	82	XX
60	22.13	6-Ethyl-1,2,3,4-tetrahydronaphthalene	30%	79	XX
61	22.17	Heptylbenzene	33%	83	x
62	22.27	3-Methyltridecane	27%	72	XX
63	22.46	1,4-Dihydro-1-methyl-3-pyridinecarbonitrile	10%	73	x
64	22.74	1-Tetradecene	90%	95	XX
65	22.90	1-Ethylnaphthalene	36%	71	XX
66	23.06	Diphenyl ether	80%	91	XX
67	23.13	1,3-Dihydro-5-methyl-2H-benzimidazol-2-one	18%	78	XX
68	23.45	1,6-Dimethylnaphthalene	38%	82	XX
69	23.51	2,3-Dimethylnaphthalene	38%	72	XX
70	23.86	3,3'-Bipyridine	9%	71	x
71	23.96	Trichloroacetic acid, hexadecyl ester	22%	73	XX
72	24.01	71(100) 43(68) 73(41) 98(31)	25%	48	x
73	24.22	2-(1-Methylethyl)naphthalene	18%	83	XX
74	24.35	92(100) 91(72) 155(32) 71(29)	4%	62	x
75	24.81	4-Methyl-1,1'-biphenyl	38%	77	XX
76	24.93	71(100) 85(76) 57(71) 43(63) 167(34)	35%	67	XX
77	24.99	1,1-Diphenyl-2-propanol	11%	80	XX
78	25.21	2-(1-Methylethyl)naphthalene	16%	79	x
79	25.35	73(100) 71(81) 43(60) 55(53) 86(22)	40%	57	XX
80	25.46	Dibenzofuran	64%	92	XX

81	26.46	135(100) 92(39) 91(36) 79(21)	23%	62	XX
82	26.79	1H-Phenalene	59%	86	XX
83	26.82	7-Hexadecene	37%	78	x
84	27.10	4,4'-Dimethylbiphenyl	9%	71	x
85	27.24	71(100) 73(69) 5(63) 57(47) 43(38)	12%	45	x
86	27.35	Isocyanatoethane	5%	77	x
87	27.66	Benzophenone	35%	77	x
88	27.75	1,2,3,4,4a,5,8,9,12,12a-Decahydro-1,4-methanobenzocyclodecene	48%	74	XX
89	27.77	9H-Xanthene	23%	70	x
90	28.54	1-Acetyl-4,6,8-trimethylazulene	59%	80	XX
91	28.64	2,6-Diisopropylnaphthalene	87%	92	XX
92	28.82	1-Acetyl-4,6,8-trimethylazulene	21%	70	XX
93	28.85	2,6-Diisopropylnaphthalene	24%	76	XX
94	29.40	1,3-Diisopropylnaphthalene	57%	82	XX
95	29.46	1-Acetyl-4,6,8-trimethylazulene	70%	83	XX
96	29.55	2,6-Diisopropylnaphthalene	74%	88	XX
97	30.44	Phenanthrene	78%	94	XX
98	34.61	213(100) 119(72) 91(44) 288(42) 135(27)	9%	46	x
99	35.57	Tetrahydropyran-Z-10-dodecenoate	8%	80	x
100	39.73	Hexanedioic acid, bis(2-ethylhexyl) ester	12%	88	XX

1. Weighted match factor as output by AMDIS with a score = 100 indicating a perfect match of an empirical spectrum with the NIST library; identification of a specific compound was only made when the weighted match factor was > ~70%, the library spectrum had unique ions and visual assessment of the mass-fragment data judged the library match to be reasonable. XX = area >100,000 counts, x = area < 100,000 counts.

Summary

The sample from Slovakia is uranium oxide, a mixture of schoepite and uraninite with an isotopic composition indistinguishable from natural uranium; no evidence for ^{236}U was detected. The relatively low impurity content together with the natural U-isotope composition suggest the sample represents a final product in the uranium fuel cycle prior to conversion to UF_6. The presence of intergrown uraninite and schoepite indicates the material was precipitated with peroxide and dried hot, ~400 ºC, but not calcined. The U isotope composition of the sample is indistinguishable from natural uranium and the compositions determined at LLNL and ITU are in excellent agreement (Table 3). The ^{234}U – ^{230}Th age of 15.5 years indicates the sample was last chemically purified in January 1997 with an uncertainty of ~2 months. The ~6 month difference between this age and that determined at the Institute for Transuranium Elements, Karlsruhe (June 1997) is just outside the limit of uncertainty given for the ITU analyses (~5 months). Additional information regarding the Th content of the sample analyzed at ITU and any differences in the application of the ^{234}U – ^{230}Th chronometer is needed to evaluate the full significance of this difference. A comparison of the properties of the Slovakian uranium oxide with samples contained in the Uranium Sourcing Database using principal components analysis,

partial least squares derivative analysis and the *iDAVE* search engine failed to produce a match, suggesting the Slovak sample was produced at a facility that is not represented in the database.

Table 9. Uranium isotope abundances measured at LLNL and ITU[1].

	LLNL Analyses		ITU Analyses	
Isotope	Atom Fraction (%)	2σ	Atom Fraction (%)	2σ
^{234}U	0.005433	0.000015	0.005410	0.00006
^{235}U	0.71962	0.00038	0.712390	0.00036
^{236}U	<0.000030		<0.000012	
^{238}U	99.275	0.014	99.2822	0.0010

1. The European Union's Institute for Transuranium Science, Karlsruhe

Appendix 1

Images of shipping containers, as received at LLNL. (A) Outermost container. (B) Inner container with intact tamper indicators. (C) Poly scintillation vial containing loose U-oxide powder. Ruler shows centimeter scale in all images.

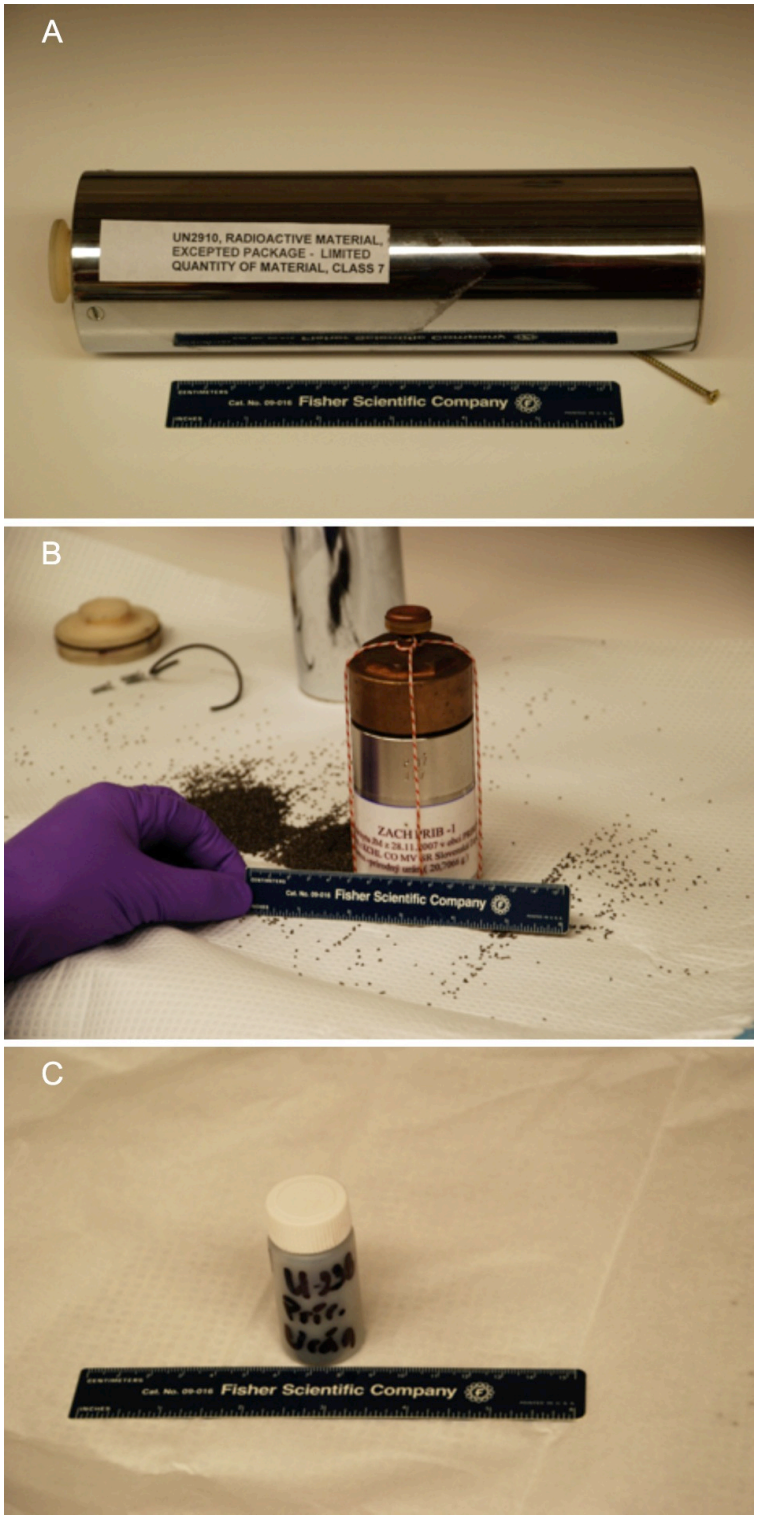

Appendix 2

PCA scores plots of the VIS-NIR data.

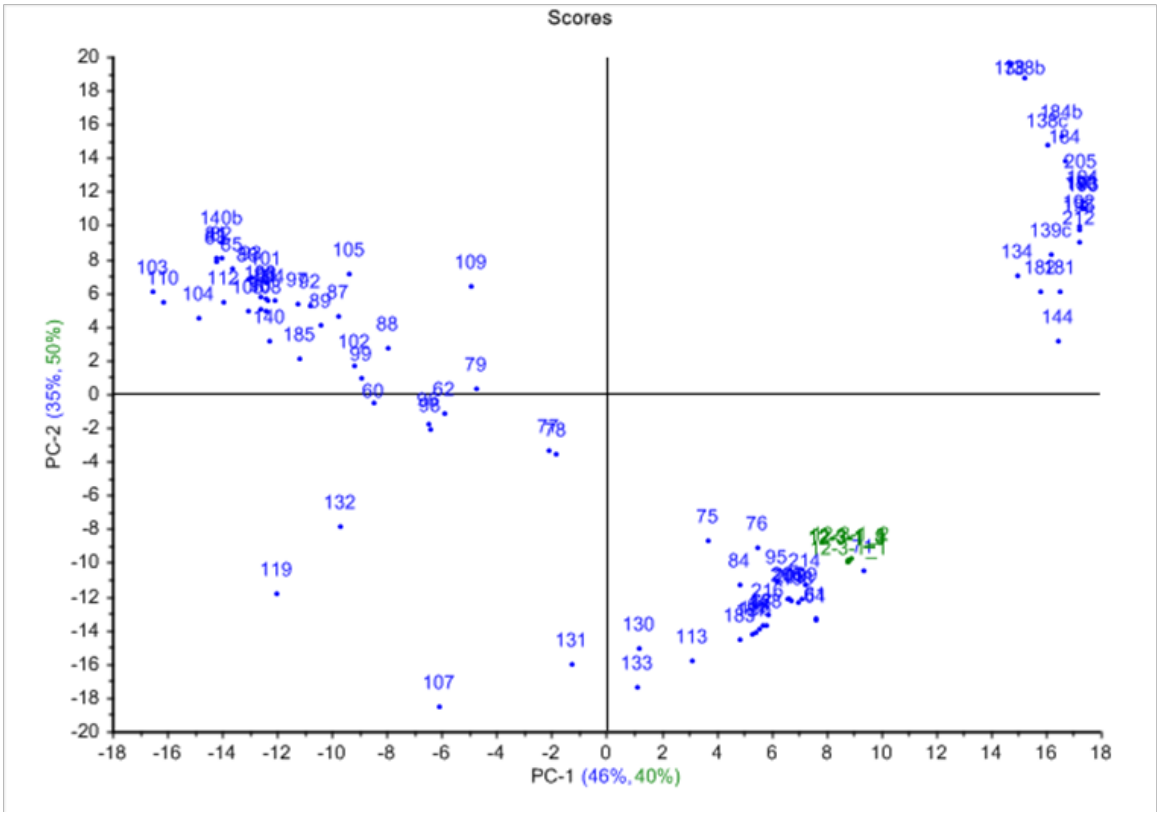

Figure 4. Projection of sample 12-3-1 on Vis+ scores plot.

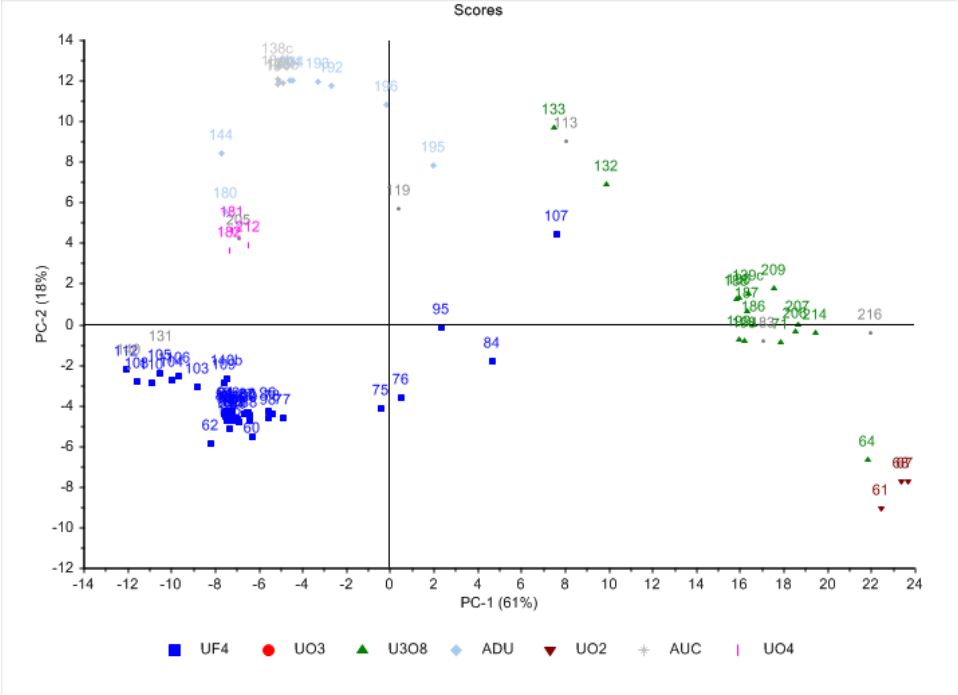

Figure 5. Scores plot of the PCA for the NIR1 range.

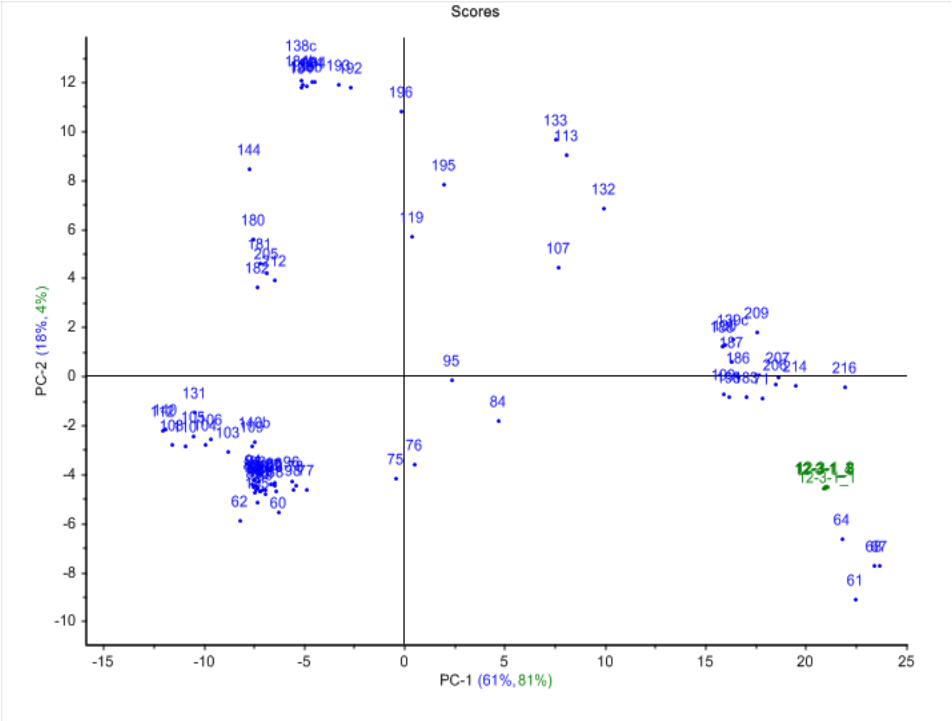

Figure 6. Projection of sample 12-3-1 on NIR1 scores plot.